Arsenic in Igneous Systems:
an experimental investigation

B.A.Sc. Undergraduate Thesis
Mike Wood

Supervisor
Dr. James Brennan

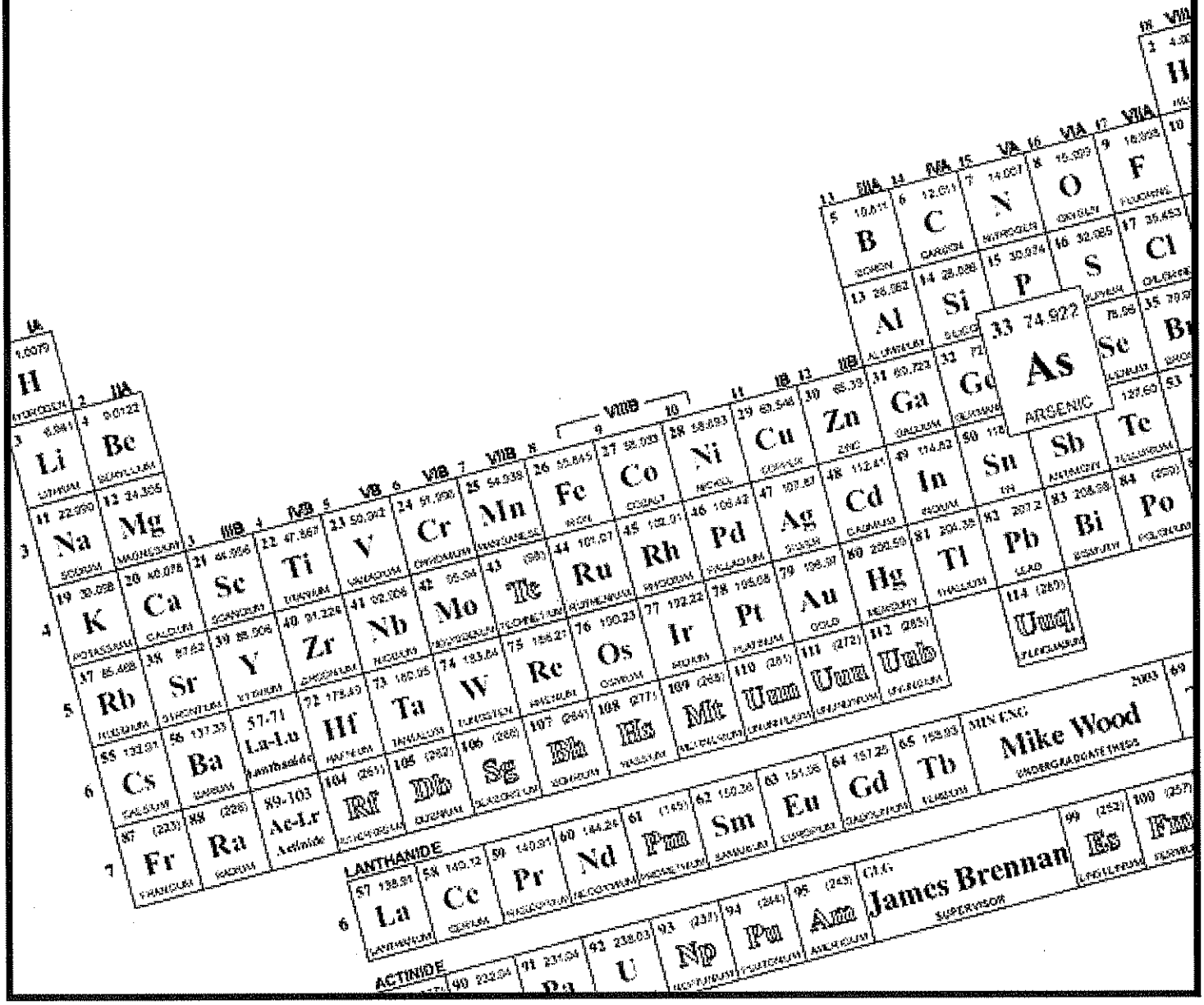

RECEIVED APR 17 2003

Table of Contents

1.0 - Introduction

Currently, the platinum group elements (PGE) are of great economic interest. Their use in automobile catalytic converters and in burgeoning, leading-edge technologies like hydrogen fuel cells has driven commodity prices to the point where geologic anomalies of PGE on the order of 1ppm have become viable resources. To date, very little quantitative research has been done regarding the concentration of these scarce elements into economic deposits. Several mechanisms for concentrating PGE in magmatic systems have been suggested, but not studied, by several authors. One such proposed hypothesis is the immiscibility of arsenic.

Studies of the mineralogy of important known PGE deposits, like the Bushveld Complex, suggest that arsenic immiscibility may play an important role in the concentration of PGE. The proposed mechanism at work is the immiscibility of arsenic in an igneous body that is slightly As-enriched but low in sulphur; the immiscible As phase collects the PGE before the melt reaches sulphur saturation (Merkle, 1991). Later textural mineralogical studies show immiscible textural relationships between sulphide and arsenide mineral globules suspended in silicate melt (Gervilla et. al, 1996). The question remains, under what conditions is arsenic immiscible?

In an effort to answer this question, an experiment was designed and conducted to measure the amount of As required to saturate a silicate melt, and to determine which melt, As or S, contains the PGE at As saturation.

2.0 - Hypothesis

Based on the study by Gervilla et al (1996), immiscibility of the arsenic phase is expected. With relation to the sulphur phase, the Gervilla photomicrographs (see figure 1) show the arsenic phase to be on the inside of the globule, showing higher surface-tension characteristics than the sulphur phase. The PGE are expected to be preferentially associated with the arsenic phase.

Figure 1

Photo A shows the sulphide pyrrhotite in an immiscible textural relationship with arsenides maucherite, nickeline, and westerveldite.

Photo B shows a similar texture, with the sulphide cobaltite clinging to the outside of a maucherite globule.

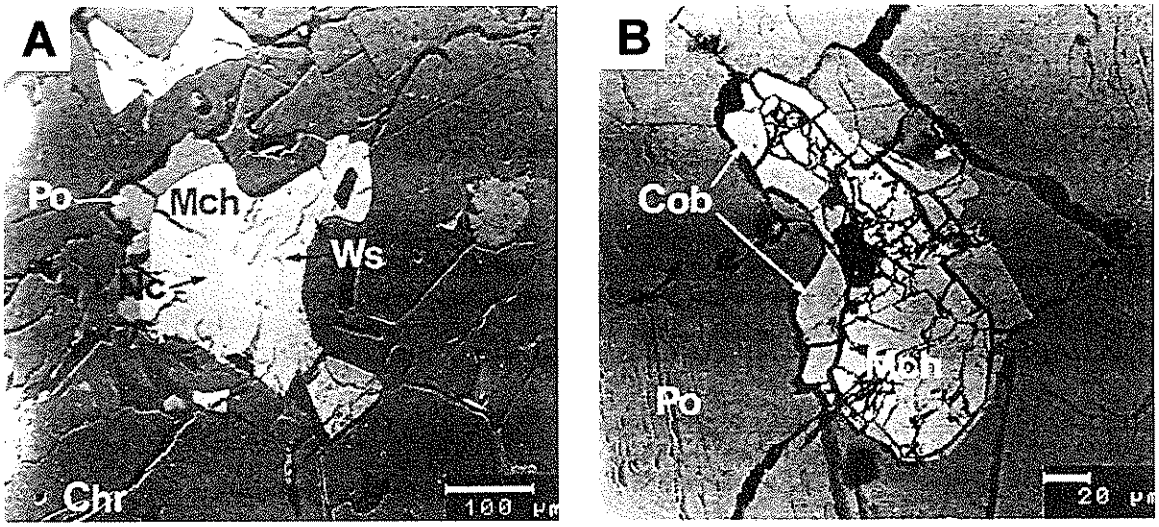

Po: pyrrhotite -- $Fe_{(1-x)}S$
Cob: cobaltite -- CoAsS
Chr: chromite -- $FeCr_2O_4$
Mch: maucherite -- $Ni_{11}As_8$
Nc: nickeline -- NiAs
Ws: westerveldite -- (Fe,Ni,Co)As

3.0 - Experimental Procedure

The objective of the experiment was to measure the solubility of As in a silicate melt, to investigate the relationship between the resulting As phase and the suite of co-existing phases, and to determine the PGE content of the As and S phases. In the experiments, only the length of the run and the content of the sample itself were varied. The temperature was maintained at a constant 1200°C, and the pressure was constant at 1GPa.

The silicate content of the samples was taken from a plateau basalt of known composition (see table 1). The samples were made from powdered reagents that were each weighed, ground in ethanol and dried to ensure homogeneity. MW-1 and MW-2 have no added Fe and as such are relatively low in Fe, closer to natural magmas (see table 2). The content of MW-3 was devised such that the molar amounts of Fe present would satisfy the stoichiometry of the equation:

$$(4.5)Fe + (0.5)Ni + As_2S_3 \Leftrightarrow 2Fe(Ni)As_{melt} + 3Fe(Ni)S_{melt}$$

Table 1

Composition of Plateau Basalt P12-623

	wt%
SiO_2	48.77
TiO_2	4.33
Al_2O_3	10.05
FeO*	12.15
MnO	0.13
MgO	7.41
CaO	10.51
Na_2O	2.60
K_2O	1.02
P_2O_5	0.48
L.O.I.	1.05
Total	98.50

Table 2

Composition of MW-1 and MW-2

	wt%
P12-623 basalt	95.00
As_2S_3	5.00
Pd	minor
Ir	minor

Table 3

Composition of MW-3
(50wt% non-basalt portion)

	mg
Fe	47.4
Ni	5.1
As_2S_3	47.0
Pd	1.4

(50wt% basalt portion)

	wt%
P12-623 basalt	50

Experimenting with arsenic at high temperatures and pressures presents serious health and safety considerations. In order to prevent the escape of arsenic into the air during the experiments, and to provide adequate delivery of temperature and pressure, the samples were contained in a multi-stage crucible/crushable sleeve assembly (see figures 2-4). The powdered sample composition was packed into (from inside out):

- a drilled-out graphite crucible 'corked' with a graphite plug.
- a relief drilled into an MgO cylinder capped with an MgO disk and an MgO cylinder with a hole to guide the thermocouple (shown pink, fig2)
- a graphite sleeve with a graphite disk at the bottom
- a pyrex glass sleeve
- a compressed NaCl sleeve

The graphite crucible is inert to the reaction in the experiment, preventing contamination of the sample. The MgO provides a crushable support for the graphite crucible, keeping the sample in the Piston Cylinder Furnace 'hot spot'. The MgO cap prevents the thermocouple from touching the conductive graphite.

The graphite, pyrex glass, and NaCl sleeves are crushable as well, and hold the assembly together. The crushable characteristics of the MgO, graphite, pyrex and NaCl mean that despite the fact that the Piston Cylinder delivers a uni-axial load, the pressure is delivered from all directions.

Figure 2

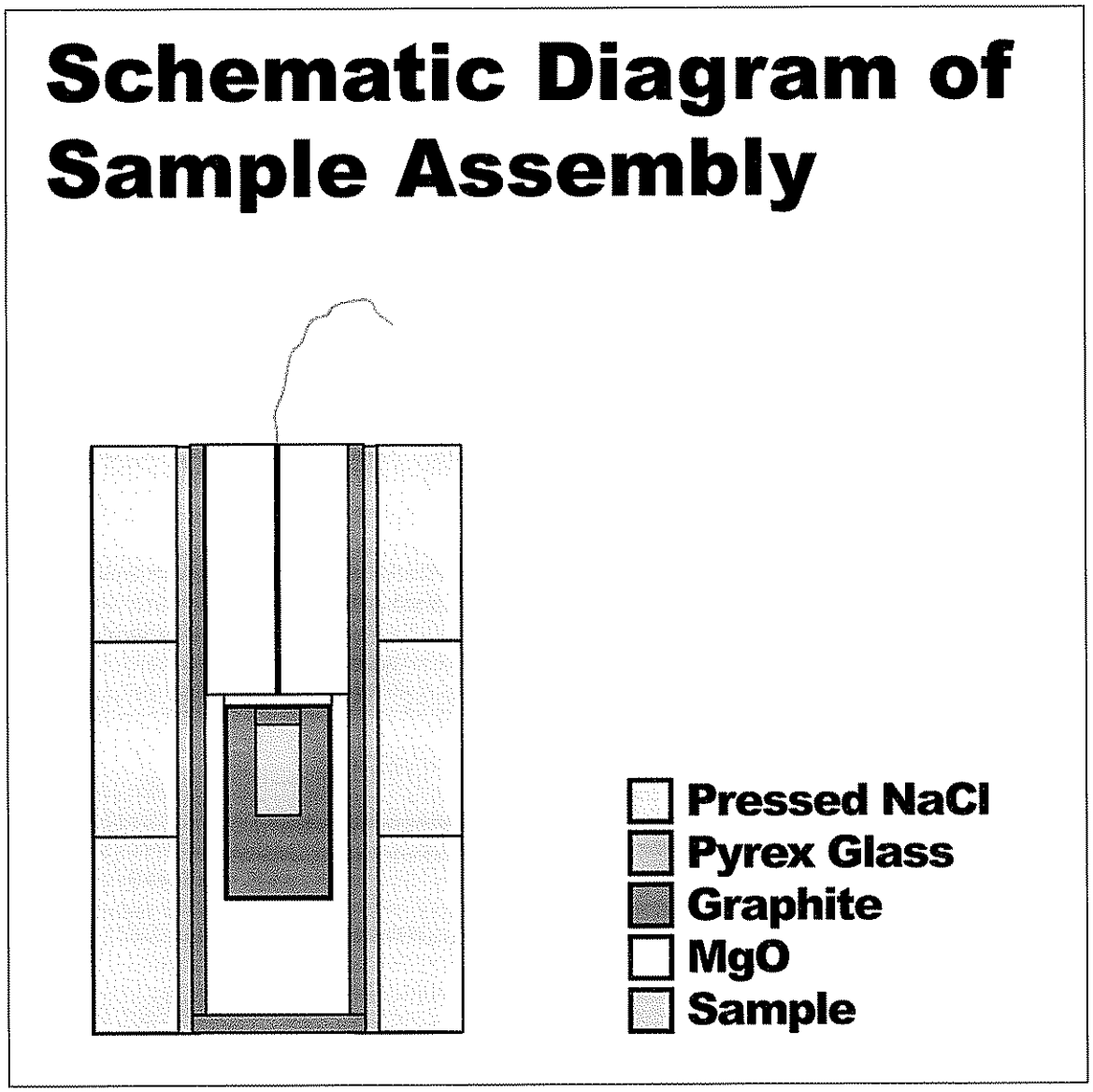
Schematic Diagram of Sample Assembly
Pressed NaCl
Pyrex Glass
Graphite
MgO
Sample

Figure 3 - Exploded View of Sample Assembly

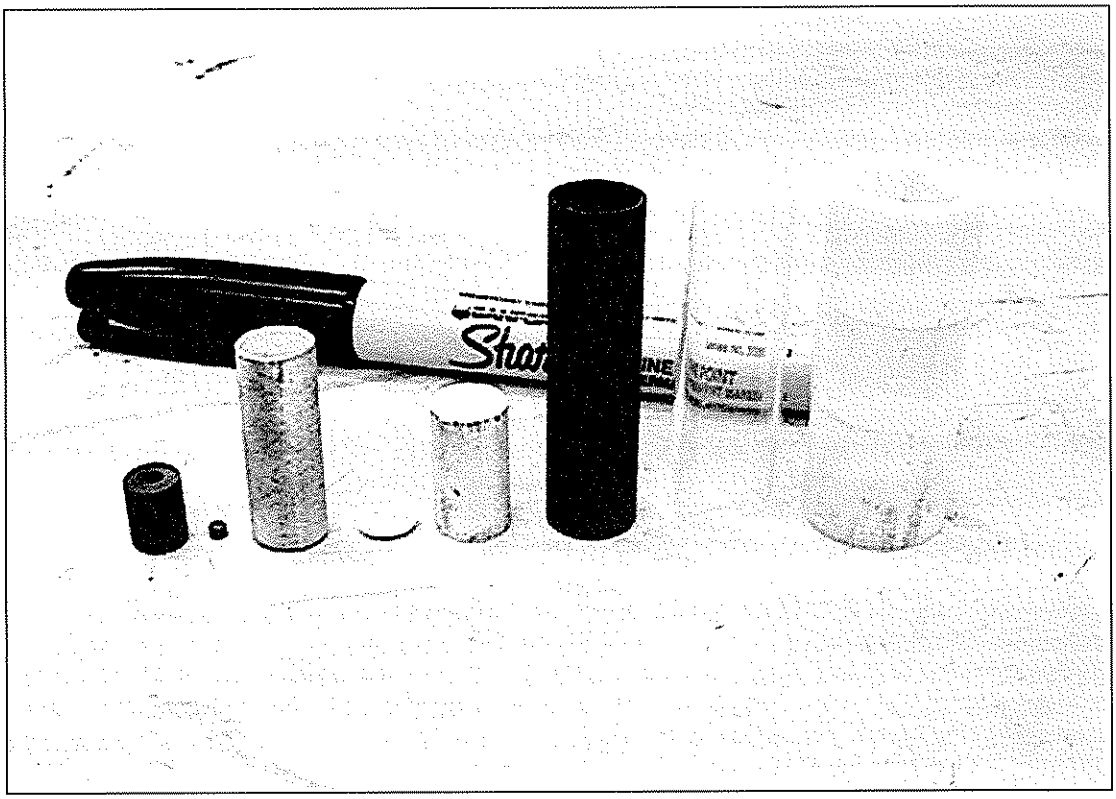

Figure 4 - Complete Assembly

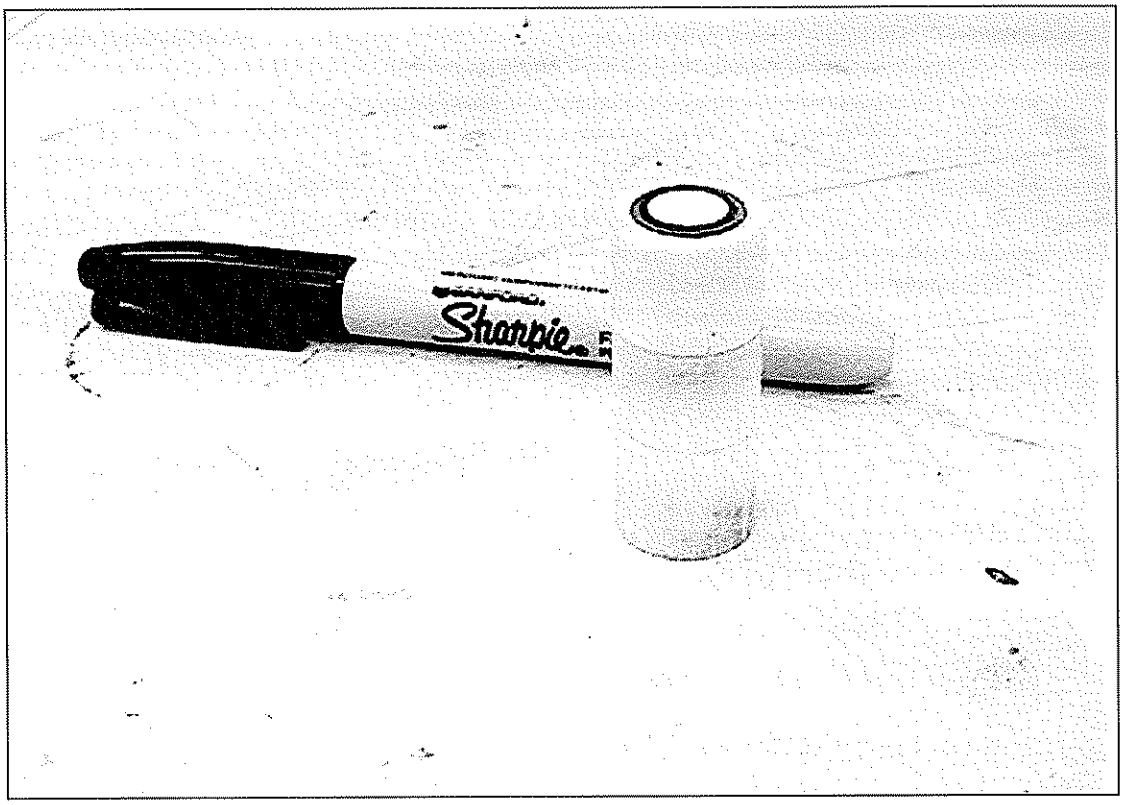

The experiments were performed in the Piston Cylinder apparatus in the High Pressure Laboratory of the Earth Sciences Building (see figures 5 & 6) which, in addition to providing the heat and pressure required, provides additional containment of the arsenic and sulphur.

Figure 5

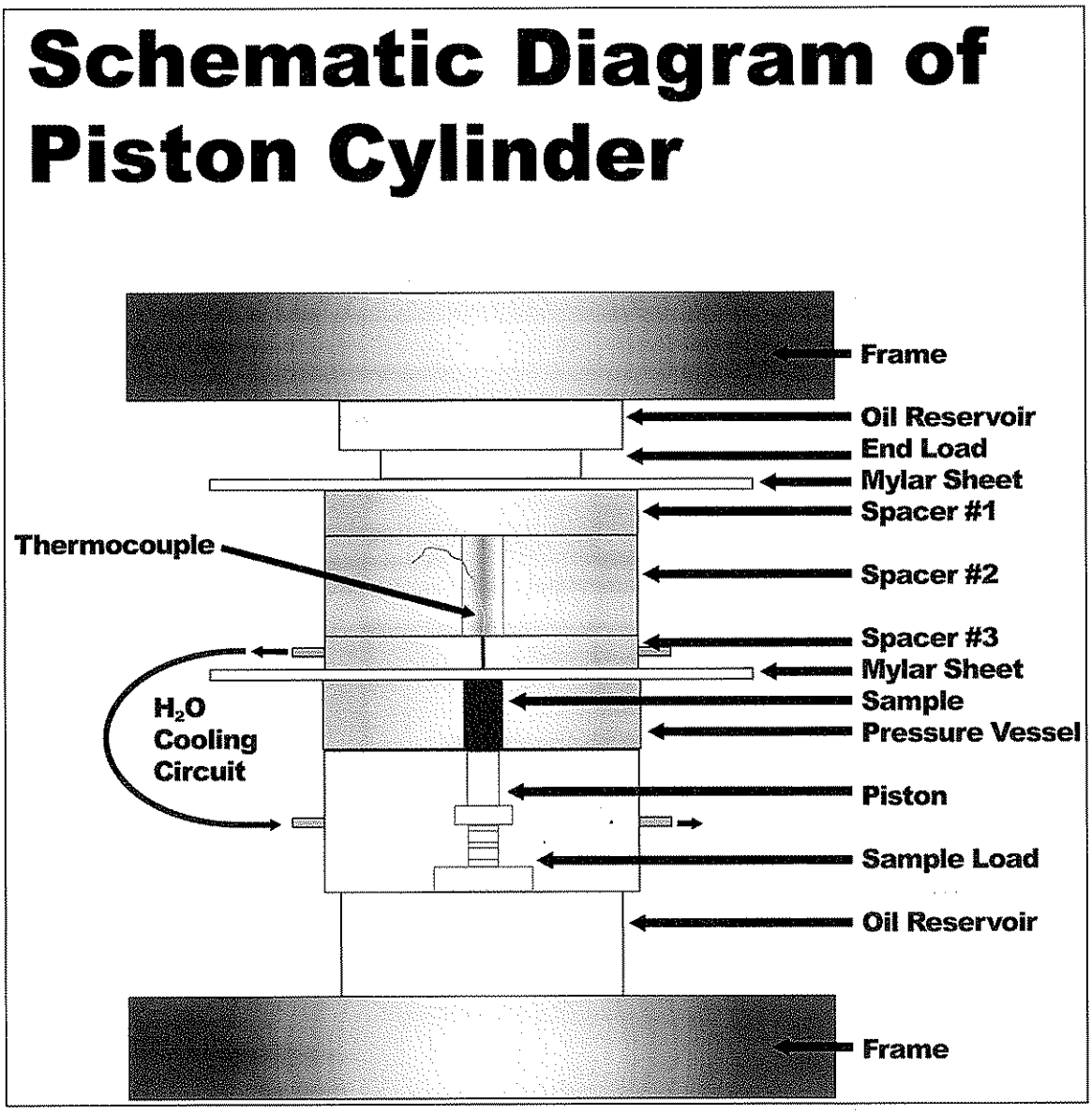

Figure 6 - Piston Cylinder

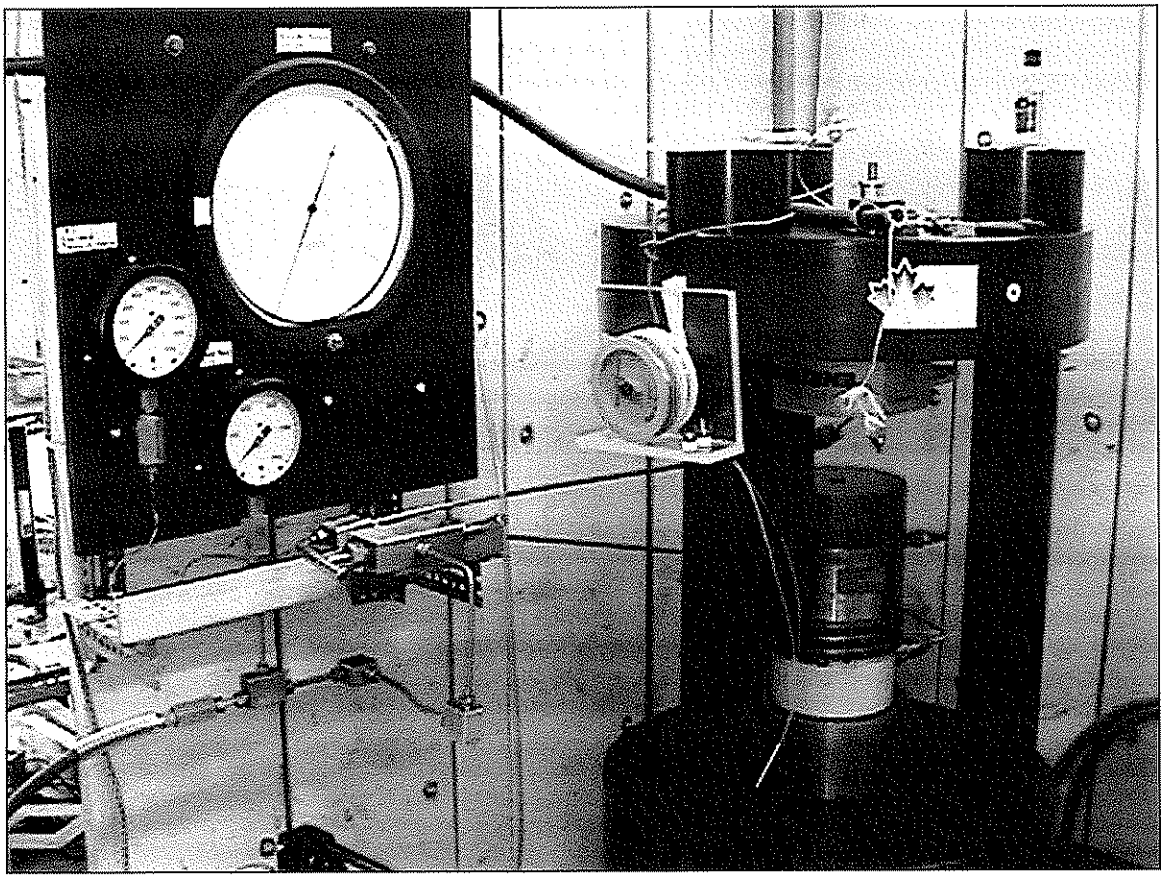

The sample assemblies MW-1, MW-2 and MW-3 were run in the Piston Cylinder for 96 hours, 48 hours, and 96 hours respectively. At the end of the runtime, each assembly was retrieved from the pressure vessel and crushed to liberate the graphite crucible and sample. Each graphite crucible was then wet-sanded to reveal the sample inside. The samples were then mounted, in epoxy, into 1" acrylic rounds. The rounds were wet-polished with coarse silicon carbide paper to further expose a section of sample, and then polished with successively finer paper down to 0.3 micron.

4.0 - Results and Analysis

Two methods of analysis were used on the run products: scanning electron microscope and electron microprobe. The JOEL JSM35 scanning electron microscope at the University of Toronto was used to investigate textures and phases present in the run products. The Cameca SX50 electron microprobe at the University of Toronto was used to analyze the major element composition of the glass and melt present in the run products.

4.1 - SEM

The scanning electron microscope investigation revealed the expected immiscibility textures and phases, as well as some unexpected textures and phases.

Figure 7 shows a sulphide/arsenide globule with obvious immiscibility textures. The darker melt is and iron-rich sulphide phase, the lighter melt is an iron-rich arsenide phase. The three main blebs in the globule are immiscible one in the other, and the smaller textural blebs are the result of quenching. The arsenic phase has a greater surface tension than the sulphur phase, which is the case throughout the experiments.

Figure 7 - Sample MW1-img3

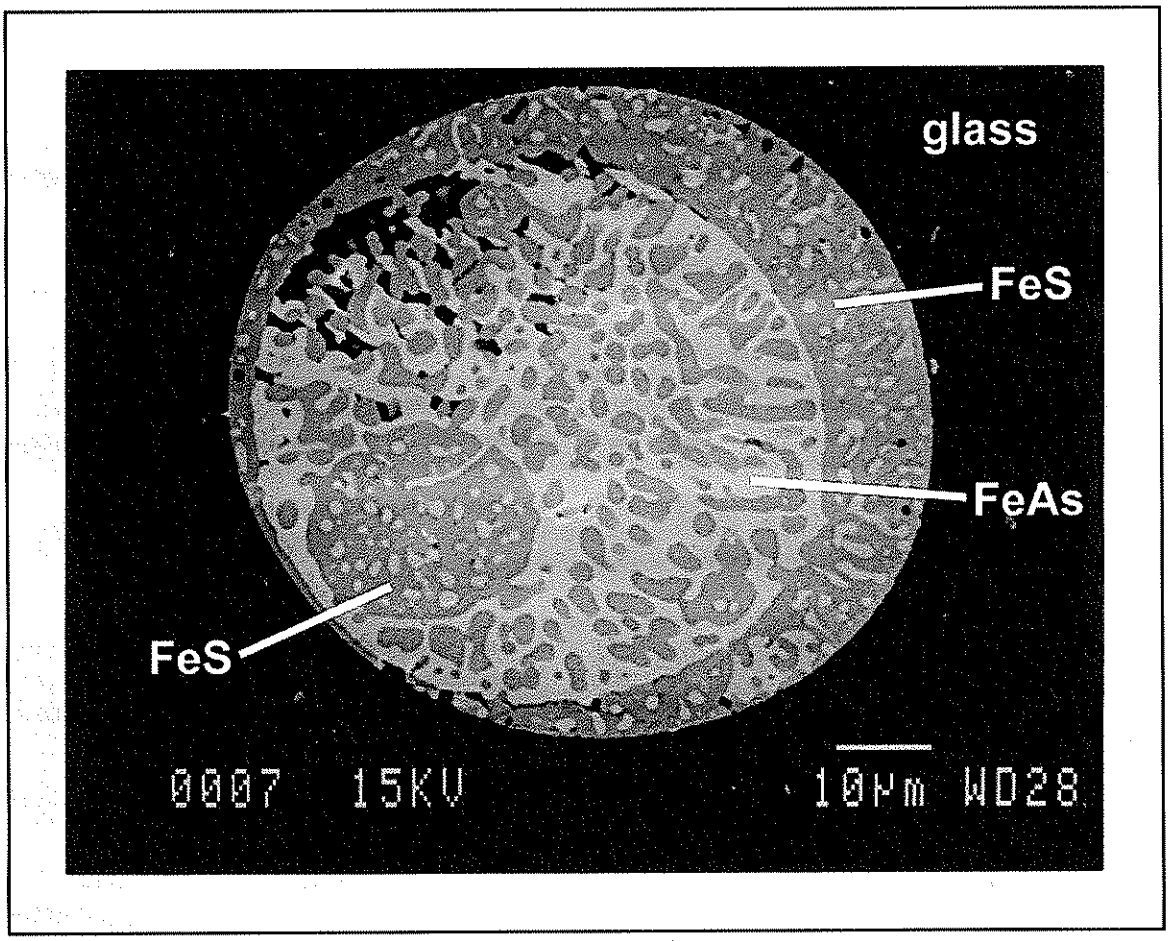

Figure 8 shows several smaller globules, each with varying content of the arsenic and sulphur phases. The fact that globules of the same size exist with varying amounts of the separate phases indicates that the immiscibility texture is not simply related to quenching or to the cross cutting relationship of the particular section through the globule in three dimensions.

Figure 8 - Sample MW1-img5

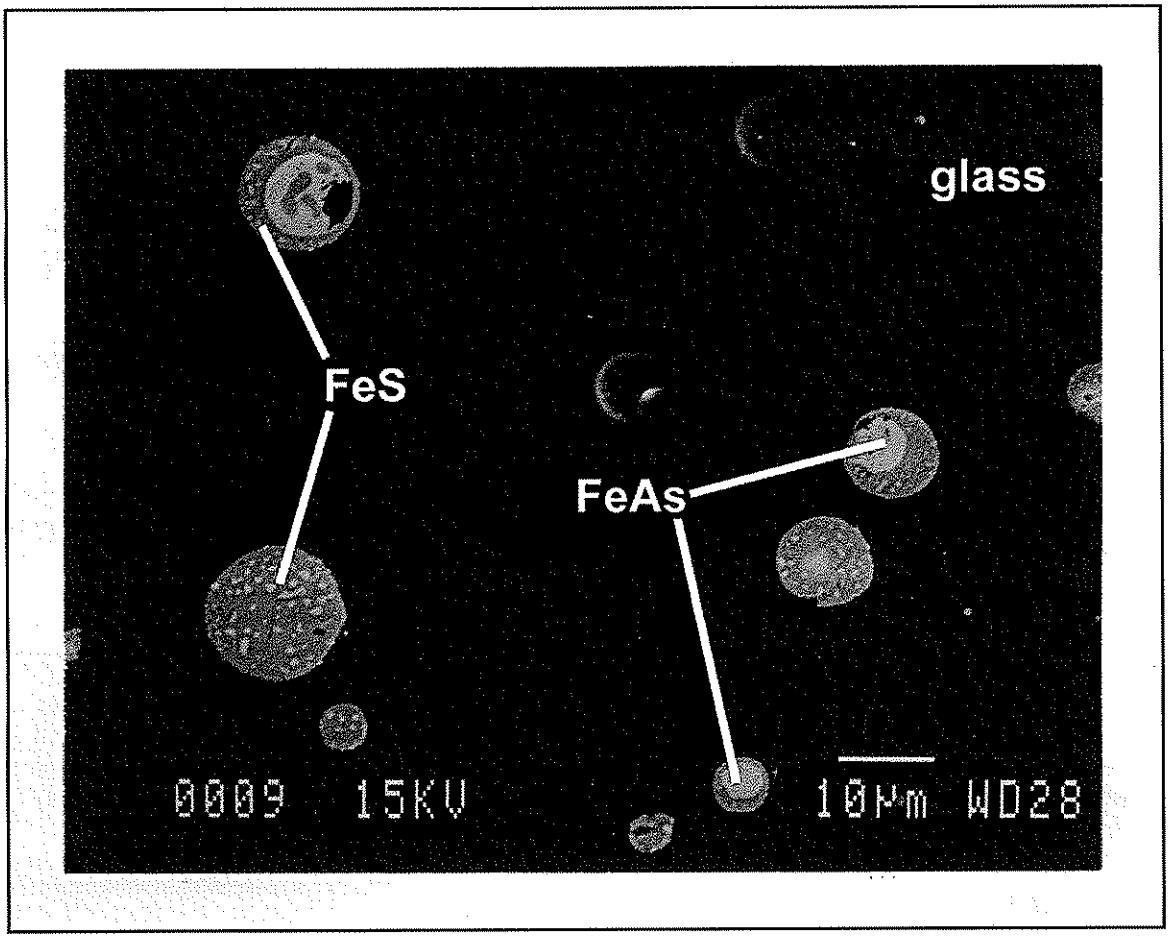

Figure 9 shows another immiscibility texture. The IrAs (iridarsenite - $IrAs_2$) crystal is surrounded by a globule of immiscible PdAs. The darker halo around the monoclinic iridarsenite crystal is likely due to As depletion of the PdAs globule as the crystal was growing.

Figure 9 - Sample MW1-img2

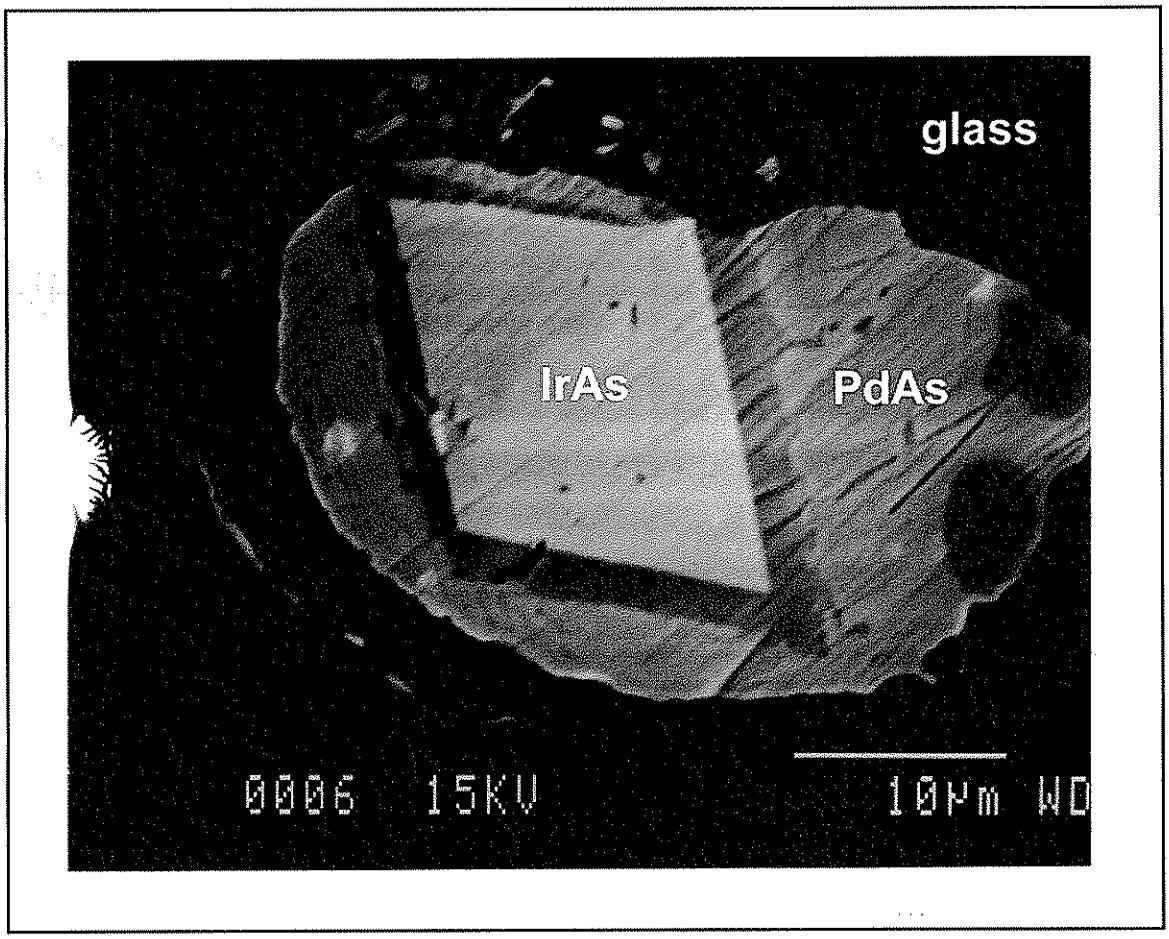

Figure 10 shows a very small globule, approximately 10µm across. This single globule contains almost every melt phase represented in the entire sample. The darker FeS half-moon has the now familiar immiscible relationship with the neighbouring arsenide phase. Inside the FeS is a very small bleb of (Fe)PdS which is immiscible in the iron sulphide phase surrounding it. The PdAs, (Pd)FeS and IrAs are also immiscible. The Ir is entirely fractionated into arsenide phases while the Pd is almost entirely fractionated into arsenide phases.

Figure 10 - Sample MW1-img1

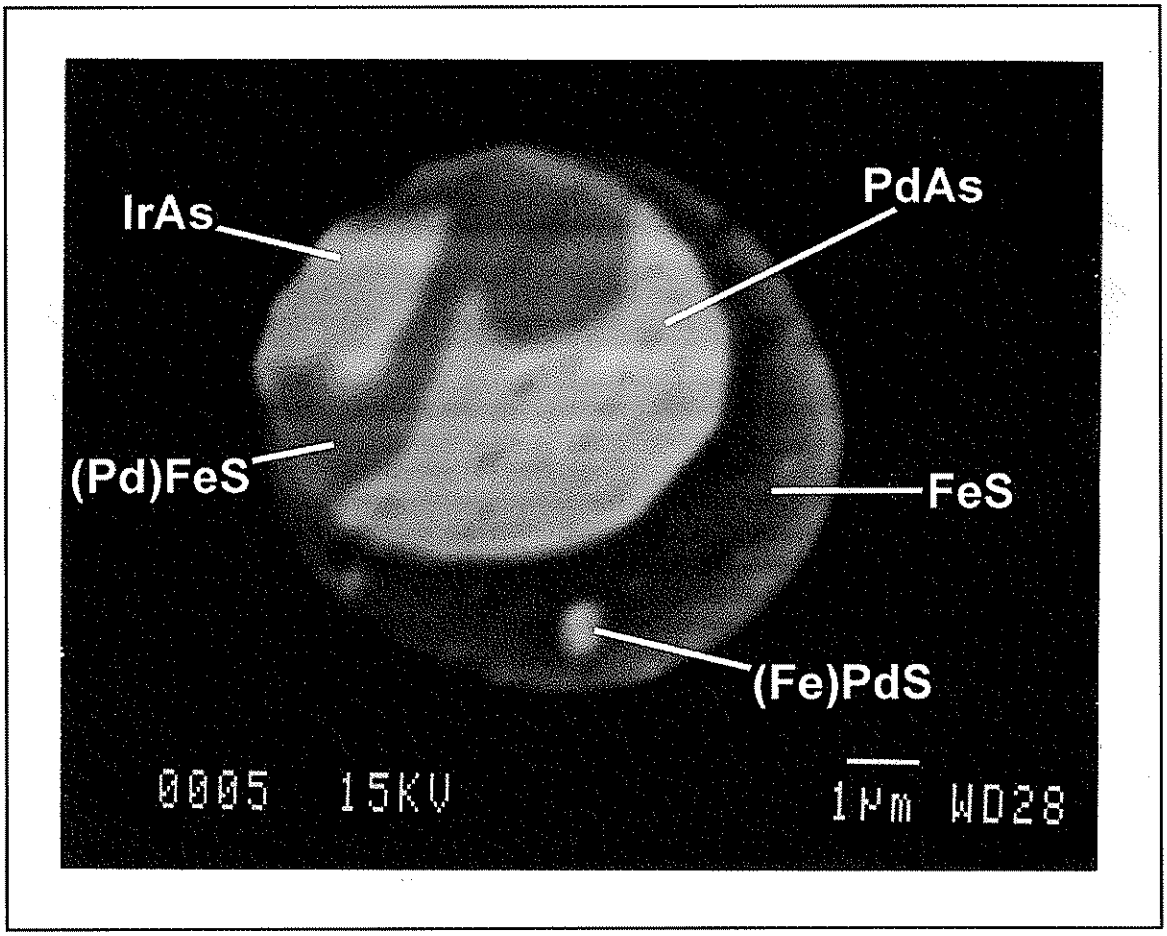

Figure 11 shows the several very large globules. During the course of the run of MW-2, the thermocouple failed. The globules pictured in figure 11 formed at unknown conditions compared to the other two runs (likely higher temperature). The same immiscibility textures are apparent as in the other samples. There are small blebs of PdS(As) present in the large dark FeS phase. The sulphur phase is outside the arsenide phase in a wetting relationship and once again, the two arsenides IrAs and PdAs(S) are immiscible. It is interesting to note that the iridium is 100% fractionated into the arsenide phase, while the palladium occurs largely in the arsenide phase, but in the sulphur phase as well.

Figure 11 - Sample MW2-img1

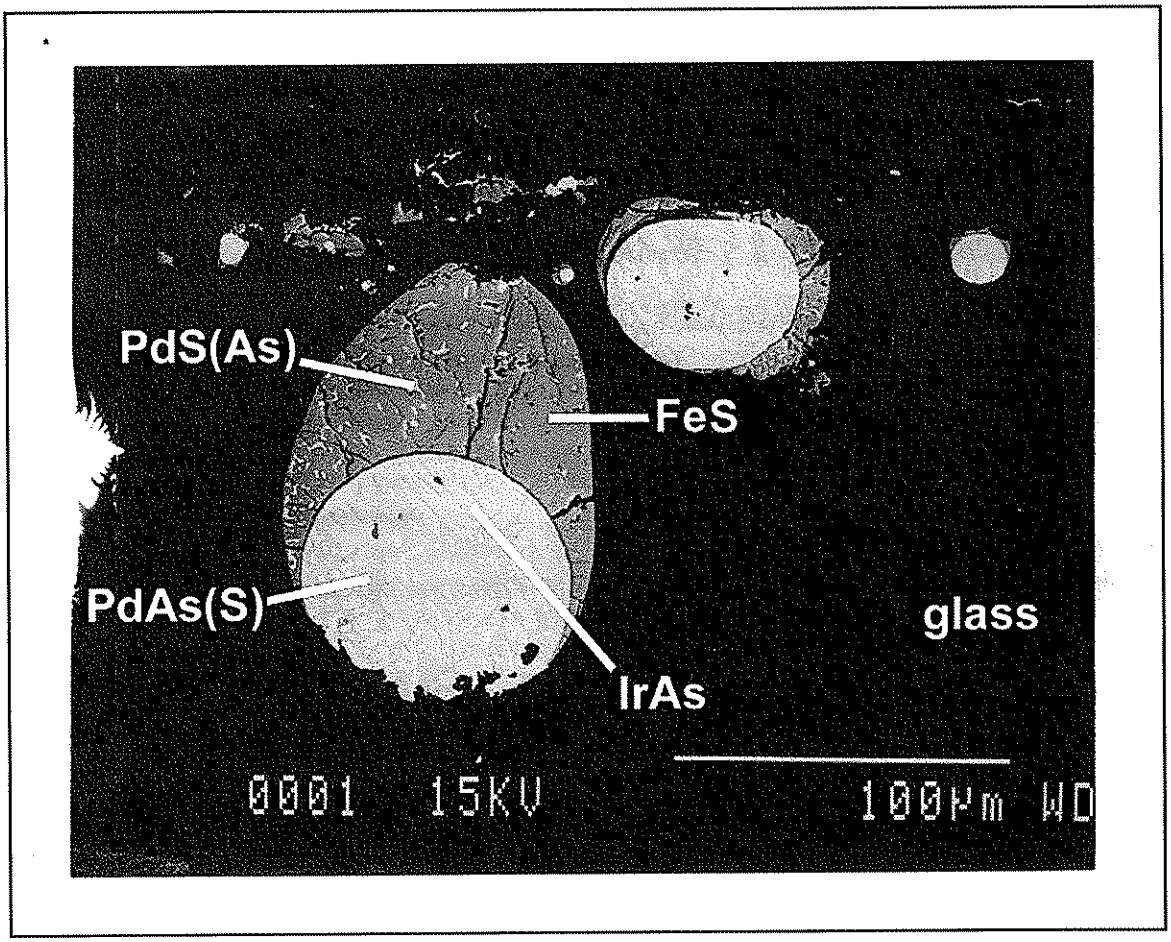

Figure 12 shows a closer view of the arsenide phase of the largest globule pictured in figure 11. The high-relief mineral is the IrAs and the darker grey is the PdAs(S).

Figure 12 - Sample MW2-img1(zoom)

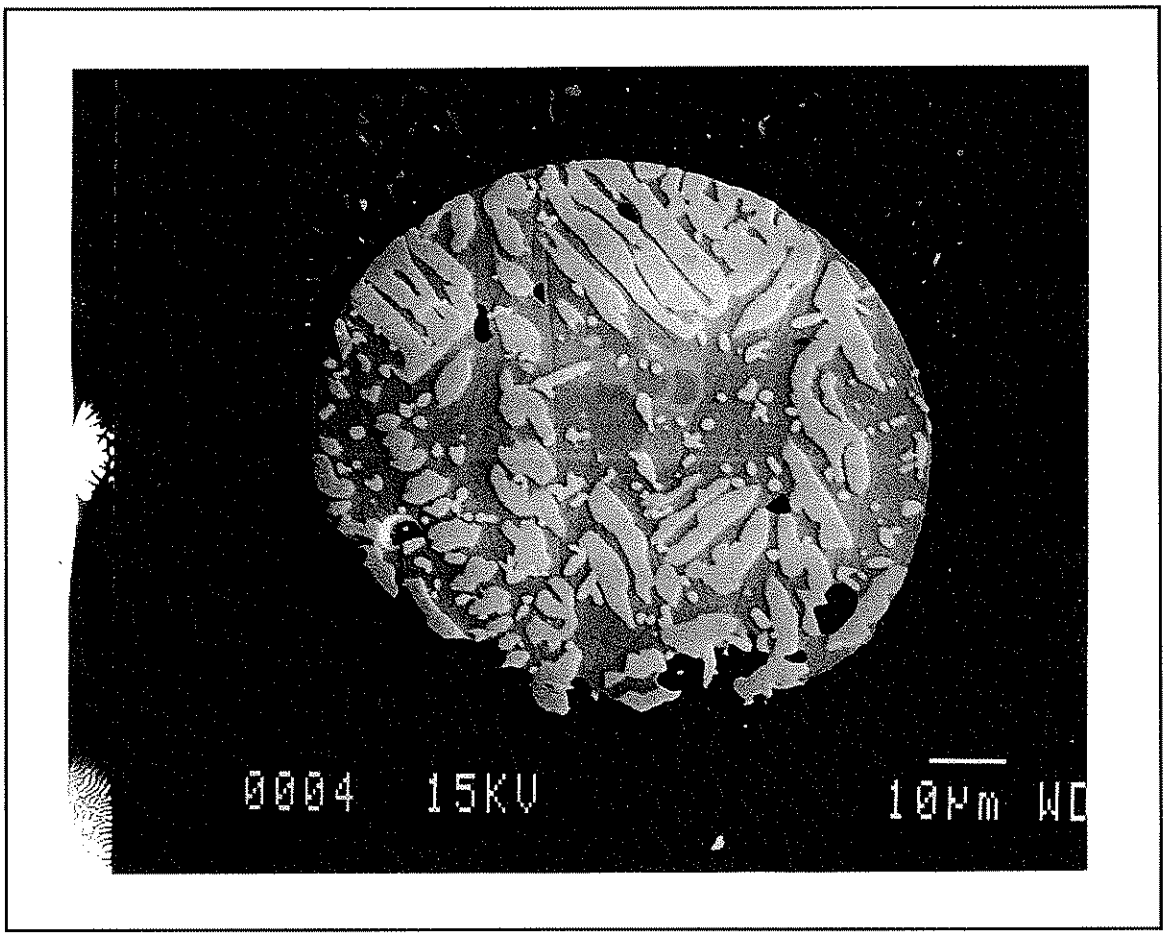

Figure 13 shows the entire sample MW-3. Surrounding the sample is the graphite of the crucible (darkest in the photo). The bright phase at the bottom of the crucible is sulphide and arsenide settled out of the sample. A silicate cumulate phase is visible as dark, almost black euhedral crystals. Sulphide and aresenide globules cling to the sides of the crucible by surface tension, and smaller globules that didn't have a chance to settle into the bottom mass are suspended throughout. MW-3 has no Pd liquid like MW-1 and MW-2. The cracks in the glass of the sample are the result of unloading the sample assembly in the piston cylinder.

Figure 13 - Sample MW3-img2

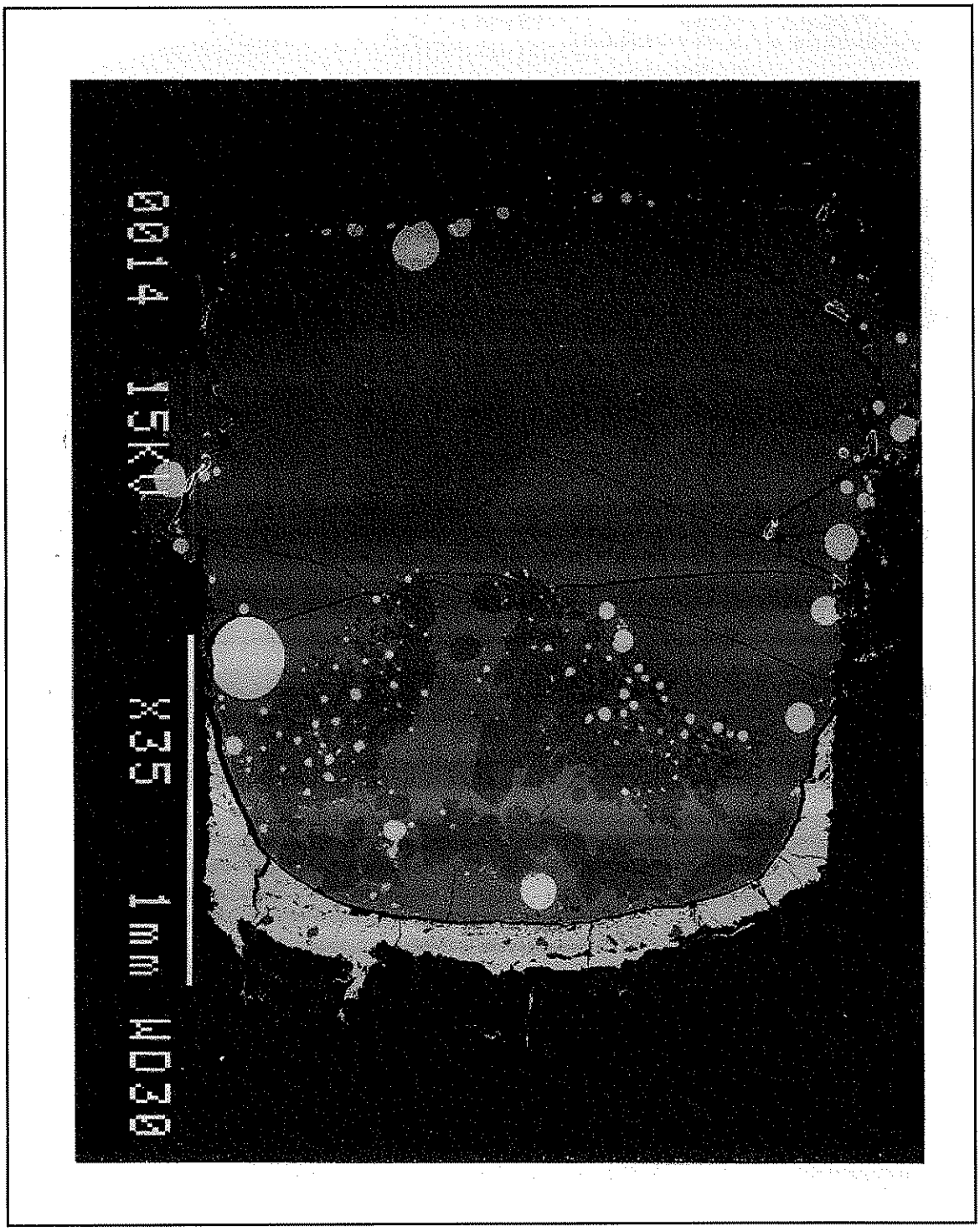

Figure 14 shows a group of sulphide and arsenide globules. They exhibit the same phase relational textures that the other samples did. The lighter coloured arsenides are wetted by the darker sulphides. Note the differences among the sulphide wetting habits; the large arsenide globule on the left has a very thin halo of sulphide and a small bleb just inside it, while the arsenide globule on the right has a large half-moon shaped sulphide mass attached to it.

Figure 14 - Sample MW3-img1

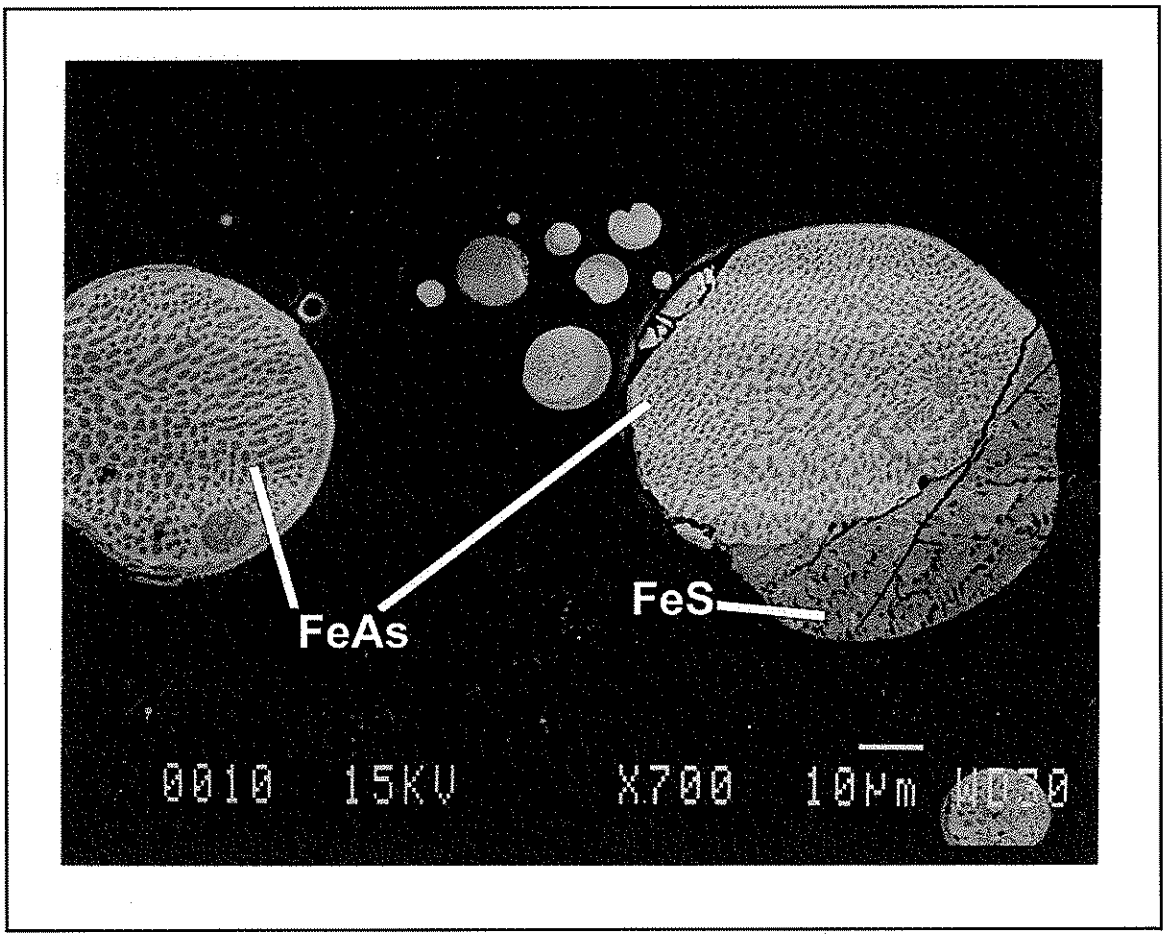

4.2 - Microprobe

The sulfide/arsenide melts in MW-3 were analyzed with an accelerating voltage of 25kV with a 30nA beam current. Analysis of the melts used different beam diameter conditions; 20µm beam diameter for the FeAs melt, and a focused spot for the FeS melt. 20-second counts were used for Fe, S, Ni, and As. Pd was counted for 60-seconds.

4.2.1 - As/S Melt Globules

In the FeS globule data (see table 4) the Pd count in the FeS is below the minimum detection limit of 270ppm. The Fe count is 10% higher in the FeS globule than it is in either of the FeAs globules.

Table 4

FeS Globules		
Element	Mean %	Standard Deviation
Fe	58.6091	1.8761
Ni	1.1788	0.6926
As	5.6682	3.6910
S	29.5325	0.8062
Pd	0.0026	0.0027
Total	94.9912	4.1834

The first of the two FeAs globules analyzed has significantly more Pd than the FeS globule (see table 5).

Table 5

FeAs Globule 1		
Element	**Mean %**	**Standard Deviation**
Fe	46.6581	0.5591
Ni	0.3001	0.3001
As	25.7700	1.0000
S	19.7322	0.6338
Pd	0.9911	0.6088
Total	98.1227	0.6072

The second FeAs globule analyzed also has significantly more Pd than the FeS globule (see table 6), but slightly less than the first FeAs globule. It also has much more Ni than either of the previous globules.

Table 6

FeAs Globule 2		
Element	**Mean %**	**Standard Deviation**
Fe	45.5206	0.8156
Ni	4.6463	0.1901
As	29.6277	2.5753
S	18.2719	1.6833
Pd	0.8411	0.3475
Total	98.9076	0.2948

As the microprobe analysis shows, Pd is quantitatively sequestered by the As-rich melt. Based on the microprobe analysis of the FeS and FeAs globules and their respective Pd contents, it is possible to calculate the partitioning of Pd between the two melts. Because the measured amounts of Pd in the sulphide are below the minimum detection limit, the amount of Pd is assumed to be 270ppm for the purposes of the calculation.

Palladium Partitioning in MW-3

$$\frac{X_{Pd}^{As}}{X_{Pd}^{S}} = \frac{0.9161}{0.0270^{*}} = 33.9$$

**minimum detection limit for Pd*

4.2.2 - Silicate Melt

The silicate melt was analyzed for As and S concentration using an accelerating voltage of 25kV, an electron beam current of 100nA, and a beam diameter of 5μm with 30 second counts.

Table 7

As & S Concentrations in Run Product Glasses						
	MW-1			MW-3		
Element	ppm	Mean %	Standard Deviation	ppm	Mean %	Standard Deviation
As	3312	0.3312	0.0275	1132	0.1132	0.0098
S	2231	0.2231	0.0034	3284	0.3284	0.0053

MW-1 is Fe-poor, and has a much higher As concentration than the Fe-rich run MW-3. From these two experiments, it would appear that As solubility is inversely tied to Fe concentration. S seems to have the reverse solubility relationship with Fe. The highest measured As solubility is 3312ppm, in MW-1.

4.2.3 - Glasses

The run glasses were analyzed for Al_2O_3, FeO, MgO, CaO, Na_2O, MnO, SiO_2, NiO, K_2O, and TiO_2 using an accelerating voltage of 15kV, an electron beam current of 10nA, and a 10µm defocused beam with 20 second counts.

MW-1 Glass Composition		
Element	**Mean %**	**Standard Deviation**
Al_2O_3	10.1774	0.2292
FeO	13.5342	0.1853
MgO	6.5546	0.1063
CaO	9.4399	0.1256
Na_2O	4.0894	0.1048
MnO	0.2189	0.0339
SiO_2	44.1687	0.6186
NiO	0.0470	0.0291
K_2O	1.8047	0.0564
TiO_2	7.0034	0.1656
Total	97.0382	0.3794

MW-3 Glass Composition		
Element	**Mean %**	**Standard Deviation**
Al_2O_3	8.7196	0.0972
FeO	18.9137	0.1749
MgO	7.1679	0.0882
CaO	10.2620	0.1118
Na_2O	3.2460	0.0717
MnO	0.2098	0.0361
SiO_2	41.5355	0.1909
NiO	0.0175	0.0378
K_2O	1.4617	0.0428
TiO_2	6.3340	0.1845
Total	97.8675	0.4781

5.0 - Discussion of Results

The highest measured As solubility is 3312ppm, in MW-1. To compare this measured solubility to natural systems, we can look at the following equation:

Arsenic Concentration for 15% Melting of Mantle

$C_{tot}^{As} = 0.05\text{ppm}$
$D_b X_{sol} = 0$
$X_m = 15\%$

$$C_m^{As} = \frac{C_{tot}^{As}}{X_m + D_b X_{sol}} = 0.333\text{ppm}$$

Using a value of 0.05ppm as the silicate earth abundance of As (McDonough, 1995), and assuming that As is a completely incompatible element ($D_b X_{sol}=0$), we see that natural systems are much lower in As than what would be required to completely saturate a melt with As. In fact, natural basalts and komatiites are significantly distant from the As concentration needed for saturation, as the histogram in figure 15 illustrates.

Figure 15

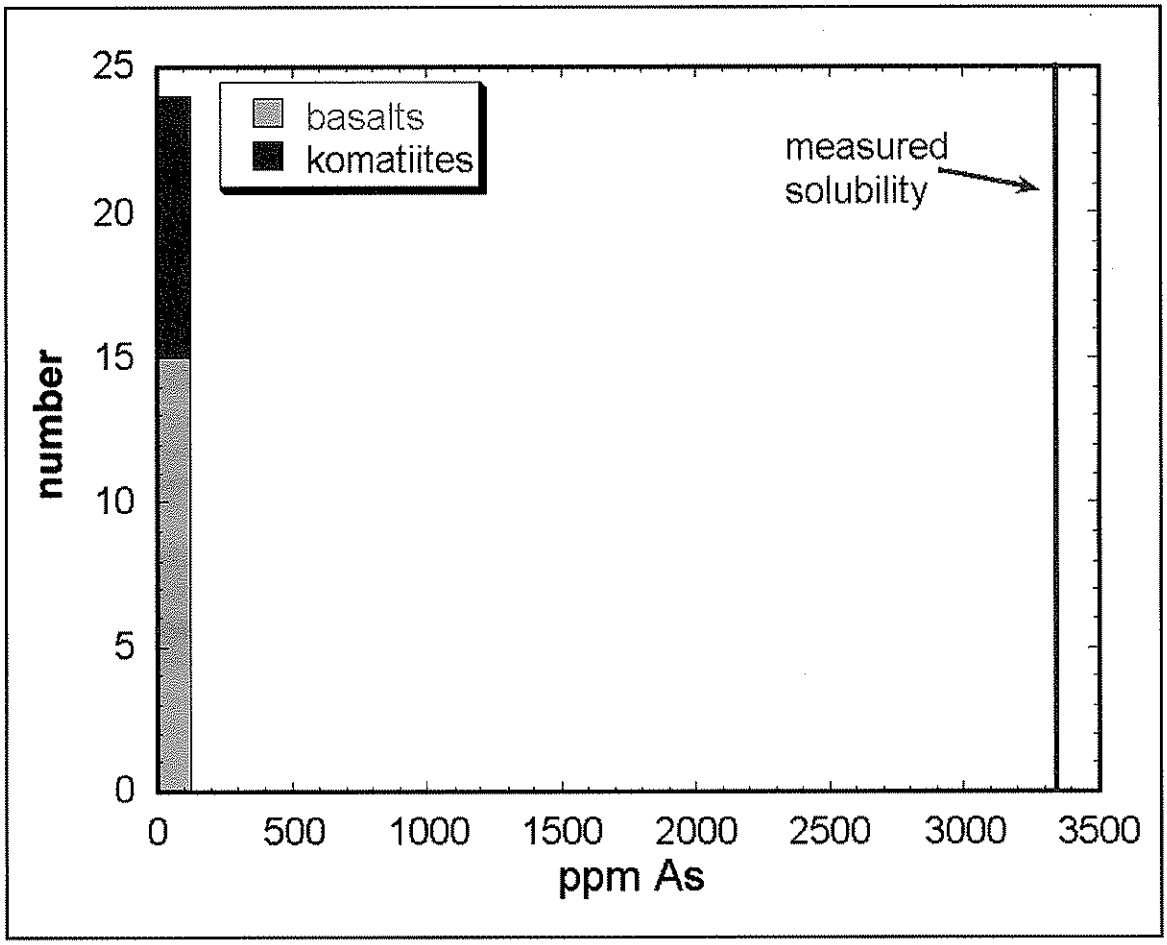
basalts
komatiites
measured
solubility
number
25
20
15
10
5
0
0
500
1000
1500
2000
2500
3000
3500
ppm As

In the same situation of 15% mantle melting, if we again assume that As is a 100% incompatible element, and allow for partial crystalization of the melt, we still can't get close to As saturation in the melt (figure 16). Even at 95% crystalization, the remaining liquid still only has an As concentration of about 16ppm.

Figure 16

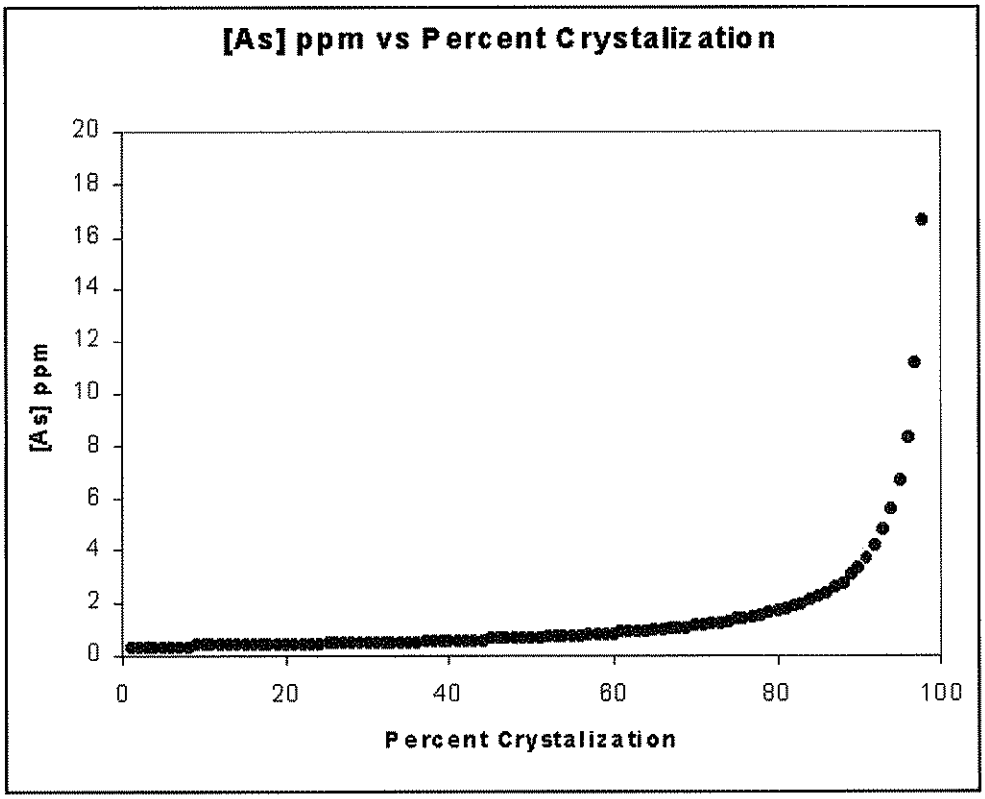

6.0 - Conclusions

Arsenic saturation of a silicate melt at 1200°C, and 1GPa is on the order of 3300ppm. The experiments also indicate that As solubility varies as an inverse function of Fe concentration. The PGE strongly prefer the As melt to the S melt; Pd by a factor of at least 34. From analysis of the experiments, it is apparent that natural magmas cannot be expected to be saturated in As.

The original interpretation of the textures seen in figure 1 (Gervilla et. al, 1996) as arsenic immiscibility at the magmatic stage, is incorrect. The textures may indeed represent immiscibility, but As saturation could not have been attained at the magmatic stage.

7.0 Recommendations

This project is an excellent launch pad for further experimentation. The results ask more questions than they answer. The most interesting question of all is "under what conditions do mobile natural magmas reach arsenic saturation?" Given the number of occurrences of PGE/arsenide mineralization, there *must* be one or more mechanisms for magma to reach As saturation. One such possibility is the assimilation of sedimentary rocks of marine origin.

Table 8 - As concentrations of sedimentary rocks (adapted from Sims et al)

	[As] ppm
Australian Post-Archean Shales	5.40
	7.30
	4.60
	10.80
	5.00
mean	6.62
Early-Archean (Greenstone Belt Shales)	14.30
	11.90
	76.00
	26.00
	17.40
mean	29.12

If magma were to come in contact with sediments with As concentrations like those listed in table 8, is it possible for the magma to reach As saturation? A thorough investigation of this possibility is certainly warranted. If complete assimilation of the arsenic present in sediments of this kind is possible, what volume of sediments must be consumed in order to saturate in As and begin sequestering PGE into an immiscible As phase, and how would the other

elemental components in the sediments affect the solubility of arsenic? The role of Fe in the S/As system is interesting, as Fe seems to affect both S and As, but in the opposite way. There might be an optimal Fe concentration at which the As concentration needed to reach saturation is lowest. As well, this project did not attempt to investigate the effects of different pressure or temperature conditions on the solubility of arsenic. Future work should determine whether P and T values play a possible role in concentrating As to saturation. The effect of fO_2 and fS_2 should be investigated, as they have an effect on sulphur solubility, so it is reasonable to assume that they have an effect on arsenic solubility as well.

References

Gervilla, F., LeBlanc, M., Torres-Ruiz, J., and Hach-Ali, P., 1996. *Immiscibility Between Arsenide and Sulfide Melts: A Mechanism for the Concentration of Noble Metals.* The Canadian Mineralogist, Vol. 34, pp 485-502

Hansen, M., 1958. *Constitution of Binary Alloys.* McGraw-Hill Book Company, Inc. New York, Toronto, London.

Makovicky, E., Karup-Moller, S., Makovicky, M., and Rose-Hansen, J., 1990. *Experimental Studies on the Phase Systems Fe-Ni-Pd-S and Fe-Pt-Pd-As-S Applied to PGE Deposits.* Mineralogy and Petrology 42, pp307-319

Makovicky, M., Makovicky, E. and Rose-Hansen, J., 1992. *The Phase System Pt-Fe-As-S at 850°C and 470°C.* N. Jb. Miner. Mh., 1992, H.10, pp 441-453; Stuttgart.

McDonough, W.F. and Sun, S., 1995. *The Composition of the Earth.* Chemical Geology 120, pp 223-253

Merkle, R., 1992. *Platinum-group minerals in the middle group of chromitite layers at Marikana, western Bushveld Complex: indications for collection mechanisms and postmagmatic modification.* Canadian Journal of Earth Science 29, pp 209-221

Sims, K.W.W., Newsom, H.E. and Gladney, E.S., 1990. *Chemical Fractionation during formation of the Earth's core and continental crust: clues from As, Sb, W, and Mo.* In: H.E. Newsom and J.H. Jones (Editors), Origin of the Earth, Oxford University Press, New York, N.Y., pp 291-317

Villars, P., Prince, A., and Okamoto, H., *Handbook of Ternary Alloy Phase Diagrams.* Vol 4. Al-Ga-Ge -- Au-Te-Tl.